J. Biochem. 2009;146(2)263–271
doi:10.1093/jb/mvp067

Biochemical and Spectroscopic Properties of Cyanide-Insensitive Quinol Oxidase from *Gluconobacter oxydans*

Tatsushi Mogi[1,2,*], Yoshitaka Ano[3], Tomoko Nakatsuka[3], Hirohide Toyama[3,†], Atsushi Muroi[4], Hideto Miyoshi[4], Catharina T. Migita[3], Hideaki Ui[5], Kazuro Shiomi[5], Satoshi Ōmura[5], Kiyoshi Kita[1] and Kazunobu Matsushita[3]

[1]Department of Biomedical Chemistry, Graduate School of Medicine, the University of Tokyo, Bunkyo-ku, Tokyo 113-0033; [2]ATP System Project, ERATO, JST, Nagatsuta, Yokohama, 226-0026; [3]Department of Biological Chemistry, Faculty of Agriculture, Yamaguchi University, Yamaguchi 753-8515; [4]Division of Applied Life Sciences, Graduate School of Agriculture, Kyoto University, Sakyo-ku, Kyoto 606-8502; and [5]Kitasato Institute for Life Sciences and Graduate School of Infection Control Sciences, Kitasato University, Minato-ku, Tokyo 108-8641, Japan

Received February 18, 2009; accepted April 9, 2009; published online May 4, 2009

Cyanide-insensitive quinol oxidase (CioAB), a relative of cytochrome *bd*, has no spectroscopic features of hemes b_{595} and *d* in the wild-type bacteria and is difficult to purify for detailed characterization. Here we studied enzymatic and spectroscopic properties of CioAB from the acetic acid bacterium *Gluconobacter oxydans*. *Gluconobacter oxydans* CioAB showed the K_m value for ubiquinol-1 comparable to that of *Escherichia coli* cytochrome *bd* but it was more resistant to KCN and quinone-analogue inhibitors except piericidin A and LL-Z1272γ. We obtained the spectroscopic evidence for the presence of hemes b_{595} and *d*. Heme b_{595} showed the α peak at 587 nm in the reduced state and a rhombic high-spin signal at $g = 6.3$ and 5.5 in the air-oxidized state. Heme *d* showed the α peak at 626 and 644 nm in the reduced and air-oxidized state, respectively, and an axial high-spin signal at $g = 6.0$ and low-spin signals at $g = 2.63$, 2.37 and 2.32. We found also a broad low-spin signal at $g = 3.2$, attributable to heme b_{558}. Further, we identified the presence of heme D by mass spectrometry. In conclusion, CioAB binds all three ham species present in cytochrome *bd* quinol oxidase.

Key words: acetic acid bacteria, cyanide-insensitive oxidase, cytochrome *bd*, Heme *d*, quinol oxidase.

Abbreviations: CIO, cyanide-insensitive oxidase; HQNO, 2-heptyl-4-hydroxyquinoline-*N*-oxide; IC_{50}, the 50% inhibitory concentration; Q_nH_2, a reduced form of ubiquinone-*n*.

Acetic acid bacteria are obligate aerobes well known as acetic acid producers and also known to oxidize various sugars and sugar alcohols such as D-glucose, glycerol, D-sorbitol, in addition to ethanol. Such oxidation reactions, which take place in the periplasm, are called oxidative fermentation, since they involve incomplete oxidation of substrates accompanied by the accumulation of oxidation products into the culture medium (*1*). Key oxidation processes are catalysed by dehydrogenases bound to the outer surface of the cytoplasmic membrane, and linked to the generation of the proton-motive force (*2*). Of this oxidative fermentation, vinegar production from ethanol and 2-keto-D-gluconate productions from D-glucose are carried out by sequential membrane-bound alcohol and aldehyde dehydrogenases and by D-glucose and gluconate dehydrogenases, respectively (*2*).

Gluconobacter is a genus of acetic acid bacteria that can oxidize a broad range of sugars, sugar alcohols and sugar acids (*3*). However, the recently released complete genome of *Gluconobacter oxydans* ATCC 621H indicates that the respiratory chain lacks complex I (NADH:quinone oxidoreductase, NDH-I), complex II (succinate:quinone oxidoreductase) and complex IV (cytochrome *c* oxidase) (*4*). Genes coding for complex III (quinol:cytochrome *c* oxidoreductase) and cytochrome *c* are identified but their functions are unclear because the absence of cytochrome *c* oxidase. NADH produced in the cytoplasm is re-oxidized by a single-subunit NADH dehydrogenase (NDH-II) bound to the inner surface of the membrane, and resultant quinols ($Q_{10}H_2$) are directly oxidized by cytochrome bo_3 oxidase (*5*) and cyanide-insensitive oxidase (CIO) (*6*). Accordingly, the growth efficiencies of these bacteria are quite low, compared to those of other aerobic bacteria. The rapid oxidation of carbon sources and the low biomass yield make acetic acid bacteria suitable for industrial applications for the bioconversion to obtain a variety of valuable products (*7*).

*To whom correspondence should be addressed.
Tel: +81-3-5841-8202, Fax: +81-3-5841-3444,
E-mail: tmogi@m.u-tokyo.ac.jp
†Present address: Department of Bioscience and Biotechnology, Faculty of Agriculture, University of the Ryukyus, Okinawa 903-0213, Japan
Correspondence may also be addressed to K. Matsushita.
Tel: +81-83-933-5858, Fax: +81-83-933-5859,
E-mail: kazunobu@yamaguchi-u.ac.jp

CIO (CioAB) is a relative of cytochrome *bd* quinol oxidase (CydAB), and has been found and described from the γ-proteobacterium *Pseudomonas aeruginosa* (*8*, *9*) and the ε-proteobacterium *Campylobacter jejuni* (*10*), both of which lack spectral features for hemes b_{595} and *d* at the dioxygen reduction site in the wild-type strains. By now, CIO has not yet been purified and the 50% inhibitory concentration (IC_{50}) for KCN and the K_m values for oxygen have been reported for enzymatic properties (*9–11*). In the opportunistic pathogen *P. aeruginosa*, which produces HCN as a metabolic product at concentrations of ~0.3 mM (*12*), CIO is used for the cyanide-insensitive respiration as well as the microaerophilic respiration. Cyanide has been detected in tissue samples infected with *P. aeruginosa* (*13*), and CIO has been shown to be required for the pathogenicity in the cyanide-mediated paralytic killing of nematodes (*14*). *Campylobacter jejuni* is a gastrointestinal pathogen and uses a cyanide-sensitive cytochrome cbb_3 oxidase [$K_m(O_2) = 40$ nM] for the microaerophilic growth in place of CIO [$K_m(O_2) = 0.8$ μM] (*10*).

Taking the advantage in the simple organization of the *G. oxydans* respiratory chain (*2*), we constructed the Δ*cioA* disruptant and CioAB-overproducing strain (wild-type/pSG-CioAB) and characterized enzymatic and spectroscopic properties of *G. oxydans* CIO in the membrane. We found that *G. oxydans* CIO was more resistant to cyanide and quinone analogue inhibitors (except piericidin A and LL-Z1272γỳ than *Escherichia coli* cytochrome *bd* and showed for the first time the spectroscopic evidence for the presence of hemes b_{558} and b_{595} and the chemical evidence for the presence of heme D (632.1 Da) bound to CIO. Our data showed that *G. oxydans* CIO binds all three hemes present in cytochrome *bd* quinol oxidase but exhibits unique spectroscopic and ligand-binding properties. We hope that future studies with the purified CIO would provide a clue for understanding the absence of spectroscopic properties in the wild-type strains.

EXPERIMENTAL PROCEDURES

Construction of the cioA Disruptant—The wild-type *G. oxydans* NBRC3172 (formerly *G. suboxydans* IFO12528) was supplied by the Institute for Fermentation (Osaka, Japan). *Gluconobacter oxydans* Δ*cioA* was constructed by the insertion of the kanamycin-resistant cassette into the *cioA* gene as follows. A *cioA* gene fragment was amplified as a 2.0-kb fragment by PCR with *PuRe Taq* polymerase (Takara Co., Tokyo, Japan) using primers, GOX0278-1 (5′-GACGCCTCATCCTTCAGGA-3′) and GOX0278-2 (5′-ATGGTTCTTACTCCGCCATG-3′), from the genomic DNA and purified PCR products were cloned into pGEM-T Easy vector. Then, at the *Bam*HI site of the *cioA* gene in the resultant vector, a 1.2-kb *Bam*HI fragment containing the Kan^R cassette from pUC4K was introduced to yield pGEM-ΔcioA. The circular pGEM-ΔcioA was directly introduced into the wild-type cells by the electroporation to perform the homologous recombination. By genomic PCR with the above primers, the disruption of the *cioA* gene in *G. oxydans* Δ*cio* was confirmed by the presence of the 3.2-kb fragment in place of the 2.0-kb fragment in the wild-type strain (data not shown).

Construction of the cioAB Expression Vector—For the over-expression of *G. oxydans* CioAB oxidase, pSG-CioAB was constructed as follows. The *Gluconobacter–E. coli* shuttle vector, pSG6, was prepared from pSG8 by the method according to Tonouchi *et al*. (*15*). The *cioAB* (*GOX0278-GOX0279*) operon was PCR-amplified as a 2.9-kb *Eco*RI–*Xho*I fragment with primers, CioAB-5′-*Eco*R1 (5′-GGAATTCTGCCGCATTGATTTTTGTCA AA-3′) and CioAB-3′-*Xho*1 (5′-CCGCTCGAGGGGCTTTT TTGTGAAGGATC-3′), from the genomic DNA using *Pyrobest* DNA polymerase (Takara Co., Tokyo, Japan). PCR products were digested with *Eco*RI and *Xho*I, and the *cioAB* operon was cloned into pSG6. The resultant pSG-CioAB was electroporated into the wild-type cells to give the overproducing strain wild-type/pSG-CioAB.

Preparation of Membrane Vesicles—Gluconobacter oxydans cells were grown aerobically in a complex media containing 20 g of sodium D-gluconate, 5 g of D-glucose, 3 g of glycerol, 3 g of yeast extract and 2 g of polypeptone per 1 l using a 50-l jar fermentor or 200 ml culture in 500-ml Erlenmeyer flasks at 30°C. Cells were harvested at the late log or stationary phase, suspended in 10 mM potassium phosphate (pH 6.0) and disrupted with a Rannie high-pressure laboratory homogenizer (model Mini-Lab, type 8.30H, Wilimington, MA) or with a French pressure cell at 110 MPa at 4°C. Membrane vesicles were recovered by centrifugation at 86,000*g* for 60 min after removal of intact cells. *Pseudomonas putida* HK5 cells were grown at 30°C in a minimal medium supplemented with 0.3% butanol. Cells were harvested at the late log phase, suspended in 50 mM Tris–HCl (pH 8.0) and disrupted by passing through a French pressure cell. After removal of intact cells, membranes were recovered by centrifugation at 86,000*g* for 90 min. The *E. coli* cytoplasmic membranes from the cytochrome *bd*-expressing strain ST4683/pNG2 (Δ*cyo* Δ*cyd*/*cyd*$^+$ Tet^R) and cytochrome bo_3-expressing strain GO103/pMFO2 (*cyo*$^+$ Δ*cyd*/*cyo*$^+$ Amp^R) were prepared, described as previously (*16*, *17*).

Enzyme Assay—Ubiquinol oxidase activity of the membrane vesicles (final concentrations of 1–10 μg/ml) was measured at 25°C in 50 mM potassium phosphate (pH 6.5) containing 0.02% Tween-20 (Calbiochem, Protein grade) with or without 1 mM KCN with a V-660 double monochromatic spectrophotometer (JASCO, Tokyo, Japan). Reactions were started by addition of 100 μM Q_1H_2 ($\varepsilon_{275} = 12.3\ mM^{-1}\ cm^{-1}$) [or 30 μM Q_2H_2 ($\varepsilon_{275} = 12.3\ mM^{-1}\ cm^{-1}$) in case of Fig. 2]. Duplicate assay was performed at each concentration and dose–response data were analysed by the non-linear curve fitting with Kaleidagraph version 4.0 (Synergy Software). The IC_{50} values were estimated as in (*18*). Enzyme kinetics was analysed by assuming the *ping-pong bi-bi* mechanism for cytochrome *bd* (*19*).

Measurements of Absorption Spectra—The membranes in the sample and reference cells with a 2-mm light path were reduced with sodium hydrosulphite and oxidized with potassium ferricyanide, respectively. Redox difference spectra were recorded in liquid nitrogen

with a Hitachi model 557 dual-wavelength spectrophotometer (*20*).

Measurements of EPR Spectra—The *G. oxydans* membranes (300 μl, 34 mg protein/ml) were placed in EPR tubes made of extra-high quality quartz (3 mm in o.d., Aguri), frozen in liquid nitrogen, and set in the cryostat (ESR900, Oxford) and EPR spectra were measured with a Bruker E500 spectrophotometer with a high-Q ER cavity.

LC-MS Analysis of Hemes—Hemes were extracted from the membranes with acetone/HCl (*21*) and dissolved in acetonitrile. The extracts were applied to a Mightysil RP-18 GP column (2.0-mm inner diameter × 100 mm, 3 μm; Kanto Chemical, Tokyo) and hemes were separated with an Aglient 1100 Series HPLC using a gradient formed from 0.4% TFA and acetonitrile (from 0 to 10 min at 20% acetonitrile, from 10 to 20 min with a 20–75% acetonitrile linear gradient and from 20 to 36 min with a 75–85% acetonitrile linear gradient) with a flow rate of 0.2 ml/min. Elution profiles were monitored by the absorbance at 405 nm with a SPD-10A_{VP} diode array detector (Shimadzu, Kyoto, Japan). Mass spectra were analysed on an API 3000 electrospray ionization mass spectrometer (Applied Biosystems) in a Q1 scan mode with the positive ion detection.

Materials—The synthesis of aurachin C 1-10 and Q_1 were described as previously (*22*, *23*). Piericidin A was a generous gift from Dr. Shigeo Yoshida (the Institute of Physical and Chemical Research, Saitama, Japan). 2-Heptyl-4-hydroxyquinoline-*N*-oxide (HQNO) and antimycin A_1 were obtained from Sigma.

RESULTS AND DISCUSSION

Identification of G. oxydans cioAB Genes—In the genome of *G. oxydans* 621H (*4*), candidates for *G. oxydans cioA* and *cioB* genes are annotated as subunit I (*GOX0278*) and II (*GOX0279*) genes, respectively, for cytochrome *bd* ubiquinol oxidase. GOX0278 (GenBank accession no. YP_190717; 53,583 Da) and GOX0279 (YP_190718; 37,813 Da) are more closely related to *cioA* and *cioB* from *P. aeruginosa* [NP_252619 (identity 59%) and NP_252618 (53%)] and *Zymomonas mobilis* [YP_163306 (67%) and YP_163307 (56%)] than *cydA* and *cydB* from *E. coli* [NP_415261 (33%) and NP_415262 (28%)] and *C. jejuni* [NP_281294 (31%) and NP_281295 (22%)], suggesting that this operon should be called as *cioAB*. To test whether these gene products are responsible for cyanide-insensitive respiration, we constructed the Δ*cioA* disruptant and the expression vector pSG-CioAB. We examined the ubiquinol oxidase activity of the membranes isolated from the stationary phase culture and found that the cyanide-insensitive quinol oxidase activity was negligible in Δ*cioA* but increased 2-fold in the overproducing strain wild-type/pSG-CioAB (Fig. 1), confirming our assignment. Cyanide-insensitive quinol oxidase activities of the stationary phase cells was ~6- and ~3-fold higher than those of the logarithmic phase cells in the wild-type and overproducing strains, respectively. Thus, as reported for *E. coli* cytochrome *bd* (*24*) and *P. aeruginosa* CIO (*8*, *9*), the expression of *G. oxydans* CIO was induced under microaerophilic growth conditions. The amount of CIO in the CioAB-overproduced membranes was estimated to be <2% of membrane proteins on the basis of SDS–PAGE analysis of subunits [1%≥ from a sum of CioA (54-kDa band) and CioB (44-kDa band) in SDS–PAGE gels; data not shown], heme B (*plus* O) content (~3%, assuming that CIO contains two *b*-hemes), V_{max} of ubiquinol-1 oxidase activity (~2%, assuming that both *G. oxydans* CIO and *E. coli* cytochrome *bd* have the similar molecular activity).

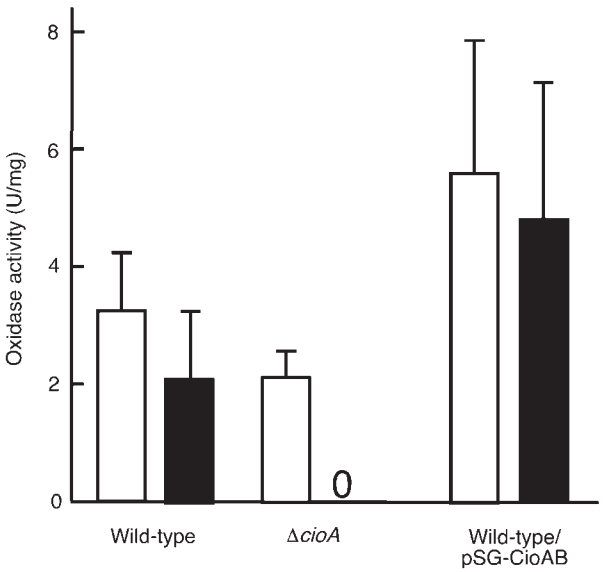

Fig. 1. **Effect of cyanide on ubiquinol oxidase activity of membranes isolated from wild-type, Δ*cioA* and wild-type/pSG-CioAB.** *G. oxydans* strains were cultured in 200 ml medium containing appropriate antibiotics in 500-ml Erlenmeyer flasks for 48 h at 30°C with rotary shaking at 200 r.p.m., and collected to prepare membrane vesicles. Oxidase activity was determined with 30 μM Q_2H_2 in the presence (filled rectangles) or absence (open rectangles) of 1 mM KCN.

Enzymatic Properties of G. oxydans CIO—Quinol oxidase activity of the membranes from the wild type showed a biphasic dependence on the KCN concentration with the IC_{50} of 8 μM (relative amplitude, 21%) and 13 mM (79%) (Fig. 2). A KCN-sensitive component showed IC_{50} comparable to 8 μM of *E. coli* cytochrome bo_3 and thus it was assigned to *G. oxydans* cytochrome bo_3. A KCN-resistant component, which was not detected in *G. oxydans* Δ*cioA* (Fig. 2), showed much a higher IC_{50} value than 1.3 mM of *E. coli* cytochrome *bd* and was assigned to *G. oxydans* CIO. We found a similar biphasic KCN concentration-dependence with *P. putida* membranes but IC_{50} of *P. putida* CIO for KCN (36 ± 32 mM) could not be unambiguously determined due to the low specific activity of CIO and the auto-oxidation of quinols at high concentrations of KCN (*i.e.* >20 mM). However, the IC_{50} value of *P. putida* is comparable to 30 mM of *P. aeruginosa* (*9*), not 3 mM reported by Cunningham *et al*. (*11*).

Kinetic properties of *G. oxydans* CIO were examined in the presence of 1 mM KCN (Fig. 3), which can completely

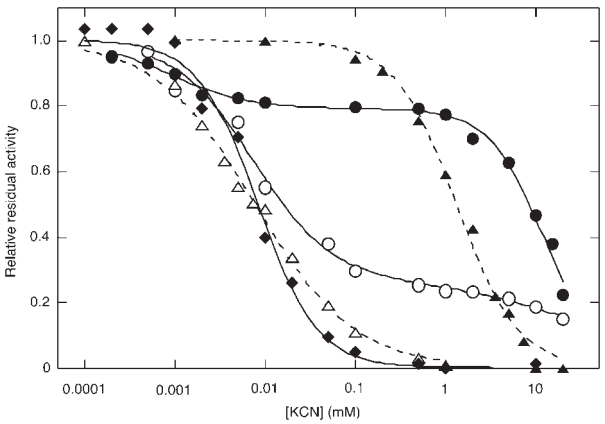

Fig. 2. **Effect of cyanide on ubiquinol oxidase activity of CIO, cytochrome *bd* and cytochrome *bo*$_3$.** Quinol oxidase activity was measured with 0.1 mM Q_1H_2 in the presence of KCN with the membranes from *G. oxydans* (wild-type and Δ*cioA*), *P. putida*, cytochrome *bd*-expressing *E. coli* ST4683/pNG2, and cytochrome *bo*$_3$-expressing *E. coli* GO103/pMFO2. Data for the wild-type *G. oxydans* and *P. putida* membranes were fitted to the two-component equation; $A_1/(1+(I/IC_{50\text{-}1})^{n1})+A_2/(1+(I/IC_{50\text{-}2})^{n2})$ where A_1 and A_2 are relative amplitudes and n_1 and n_2 are the Hill coefficients. IC_{50} values for KCN were determined to be 8.4 μM (taken from the value in Δ*cio*; 21%) and 12.6 ± 0.7 mM (79%) for *G. oxydans* WT membranes (filled circle) and 7.5 ± 1.3 μM (73%) and 35.5 ± 31.5 mM (27%) for *P. putida* membranes (open cirlce). Data for membranes from *G. oxydans* Δ*cio* and *E. coli* were fitted to the single component equation, and IC_{50} values were determined to be 8.4 ± 0.7 μM for *G. oxydans* Δ*cio* (filled diamond), 1.34 ± 0.07 mM for *E. coli* cytochrome *bd* (filled triangle) and 7.8 ± 0.4 μM for *E. coli* cytochrome *bo*$_3$ (open triangle).

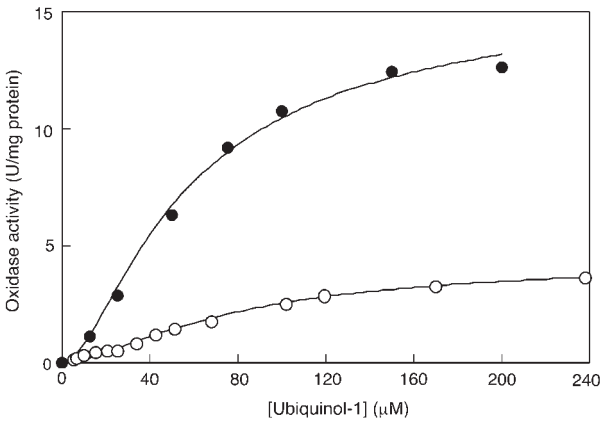

Fig. 3. **Kinetic analysis of the ubiquinol-1 oxidase activity of *G. oxydans* CIO and cytochrome *bo*$_3$.** Quinol oxidase activities of CIO and cytochrome *bo*$_3$ were measured with the membranes isolated from *G. oxydans* wild type (in the presence of 1 mM KCN) and *G. oxydans* Δ*cioA*, respectively. Apparent V_{max} and K_m values were estimated to be 16.3 ± 0.5 U/mg protein and 40.3 ± 2.5 μM, respectively, for CIO (closed circle), and 4.7 ± 0.2 U/mg protein and 55.2 ± 2.9 μM, respectively, for cytochrome *bo*$_3$ (open circle). One U was defined as 1 μmol ubiquinol-1 oxidized/min.

suppress the cytochrome *bo*$_3$ activity. The dependence of the oxidase activity on the Q_1H_2 concentration exhibited the sigmoidal behavior (Fig. 3), as found for *E. coli* cytochrome *bd* (*19*, *25*). Thus, data were analysed based on the modified *ping-pong bi-bi* mechanism (*19*). The apparent K_m value for Q_1H_2 was estimated to be 40 μM, which is comparable to 56 μM of *E. coli* cytochrome *bd* (*25*), suggesting the similarity in the ubiquinol-binding site between CIO and cytochrome *bd*. Kinetic properties of cytochrome *bo*$_3$ quinol oxidase in *G. oxydans* Δ*cioA* were examined in the absence of KCN. Data were fitted to the *ping-pong bi-bi* kinetics and the apparent K_m value was determined to be 55 μM (Fig. 3), comparable to 30 μM of *P. putida* cytochrome *bo*$_3$ (data not shown) and 50 μM of *E. coli* cytochrome *bo*$_3$ (*26*).

Identification of Quinol-Binding Site Inhibitors for CIO—For the identification of CIO-specific inhibitors, we carried out the screening of the Kitasato Institute for Life Sciences Chemical Library (*27*). From the screening of a total of 304 microbial compounds at final concentrations of 5 μg/ml with the *G. oxydans* wild-type membranes, we found the weak inhibitory activities on 0.1 mM Q_1H_2 oxidase activity with the known *E. coli* cytochrome *bd* inhibitors (*28–31*); antimycin A (residual activity, 56%), cyclic decapeptide gramicidin S (67%) and prenylphenol LL-Z1272γ (69%). Prenylphenol ascofuranone, a potent inhibitor for *Trypanosoma* alternative quinol oxidase (*30*, *32*), did not show the inhibitory activity. Then we extended our screening to the laboratory stock of quinone-analogue inhibitors at final concentrations of 10 μM and identified aurachin C 1-10 (residual activity, 15%), aurachin D 5-10 (16%) and piericidin A (14%) as potent inhibitors for *G. oxydans* CIO.

Determination of IC50 Values for CIO Inhibitors—By using the *G. oxydans* wild-type membranes in the presence of 1 mM KCN, we determined the IC_{50} values for aurachin C 1-10 (0.4 μM), piericidin A (0.7 μM), HQNO (13 μM), LL-Z1272γ (13 μM), antimycin A (17 μM) and gramicidin S (40 μM) (Fig. 4). In contrast to *G. oxydans* CIO, *E. coli* cytochrome *bd* was more sensitive to quinolone inhibitors aurachin C 1-10 (9 nM) and HQNO (0.7 μM), antimycin A (6 μM) and gramicidin S (3 μM), but less sensitive to piericidin A (8 μM) and LL-Z1272γ (57 μM) (*31*). These results emphasized the difference in the inhibitor-binding site(s) between CIO and cytochrome *bd*.

Visible Spectroscopic Properties of G. oxydans CIO—Due to the difficulty in the purification of CIO, enzymatic and spectroscopic properties of CIO remain obscure. *Gluconobacter oxydans* CIO oxidase was also unstable and most of cyanide-insensitive quinol oxidase activity was lost upon solubilization with non-ionic detergents like sucrose monolaurate. Accordingly, we examined low-temperature redox difference spectra of the membranes to find spectral features attributable to CIO (Fig. 5). The membranes isolated from the wild-type/pSG-CioAB, Δ*cioA* and wild type all showed a predominant peak at 552.5–553 nm for ferrous heme *c*, which is mainly due to the heme *c* of quinoprotein alcohol dehydrogenases present at a large amount in these strain (*6*, *33*). As reported for *P. aeruginosa* (*8*) and *C. jejuni* (*10*), the spectral differences between the wild type and Δ*cioA* were insignificant. In contrast, the CioAB-overproduced membranes from the wild-type/pSG-CioAB

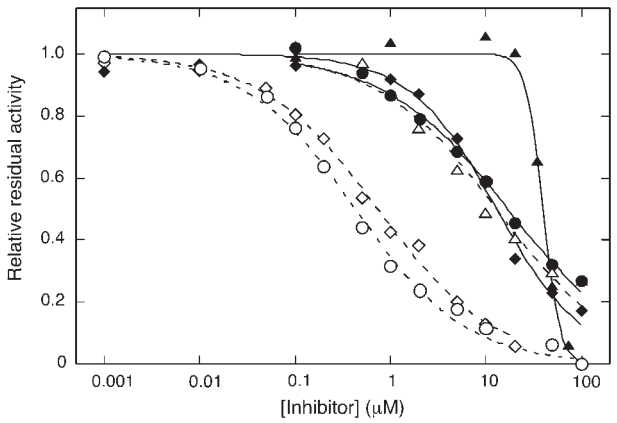

Fig. 4. **Dependence of oxidase activity of *G. oxydans* CIO on the inhibitor concentration.** In the presence of aurachin C 1-10 (open circle), piericidin A (open diamond), HQNO (open triangle), antimycin A (filled circle), LL-Z1272γ (filled diamond) or gramicidin S (filled triangle), quinol oxidase activity of membranes were measured with 0.1 mM ubiquinol-1. Data points were average values from duplicate assay. *Gluconobacter oxydans* CIO (*G. oxydans* membranes in the presence of 1 mM KCN). IC_{50} values were estimated to be 0.43 ± 0.03 (aurachin C 1-10), 0.74 ± 0.05 (piericidin A), 13.0 ± 2.0 (HQNO), 17.1 ± 1.3 (antimycin A), 13.2 ± 1.1 μM (LL-Z1272γ) and 40.1 ± 0.9 μM (gramicidin S).

increased the heme B (*plus* O) content 2-fold and exhibited the α peak for heme b_{595} at 587 nm and for heme *d* at 626 (d^{2+}) and 644 (d^{2+}-O_2) nm. Upon addition of 1 mM KCN, the ferrous heme *d* peak shifted from 626 nm to 617 nm nm (data not shown). In the *P. aeruginosa* CIO-overproduced membranes, heme *d* has been identified at 623 (d^{2+}) and 645 (d^{2+}-O_2) nm (*8*). Thus, spectroscopic properties of the CIO heme *d* are similar to those of *E. coli* cytochrome *bd* [627 (d^{2+}) and 650 (d^{2+}-O_2) nm] (*34*).

EPR Properties of the G. oxydans CioAB-over Produced Membranes—EPR studies on cytochrome *bd* from *E. coli* and *Azotobacter vinelandii* have identified that hemes *d* and b_{595} exhibit the axial high-spin $g = 6.0$ signal and the rhombic high-spin signal with $g_{y,z} = 5.5$ and 6.3, respectively (*35–38*). A rhombic low-spin species with $g_{x,y,z} = 1.85$, 2.3 and 2.5 has been assigned to a minor population of the axial high-spin species (*38–40*). Further, the low-spin $g_z = 3.3$ signal has been assigned to heme b_{558}.

We determined EPR spectra of the *G. oxydans* membranes from the CioAB-overproduced strain and Δ*cioA* mutant (Fig. 6) and calculated the CioAB-overproduced *minus* Δ*cioA* difference spectrum (Fig. 6C), by assuming that the contents of other cytochromes like alcohol dehydrogenases are similar in the both membranes. The difference spectrum representing properties of *G. oxydans* CIO were similar to that of the *E. coli* cytochrome *bd*-overproduced membranes (*38*) (Fig. 6C). Further, the $g = 3.4$, 2.46 and 2.32 signals of *E. coli* cytochrome *bd* may be shifted to $g = 3.2$, 2.37 and 2.32, respectively, in *G. oxydans* CIO and we found the $g = 2.73$ and 2.63 low-spin signals with the unknown origins. Notably, Tsubaki *et al*. (*40*) observed similar signals at $g = 3.15$, 2.96 and 2.82 in the CN-bound form of *E. coli* cytochrome *bd*. Our observations indicate that *G. oxydans* CIO contains hemes with the EPR properties similar to hemes b_{558}, b_{595} and *d* present in *E. coli* cytochrome *bd*.

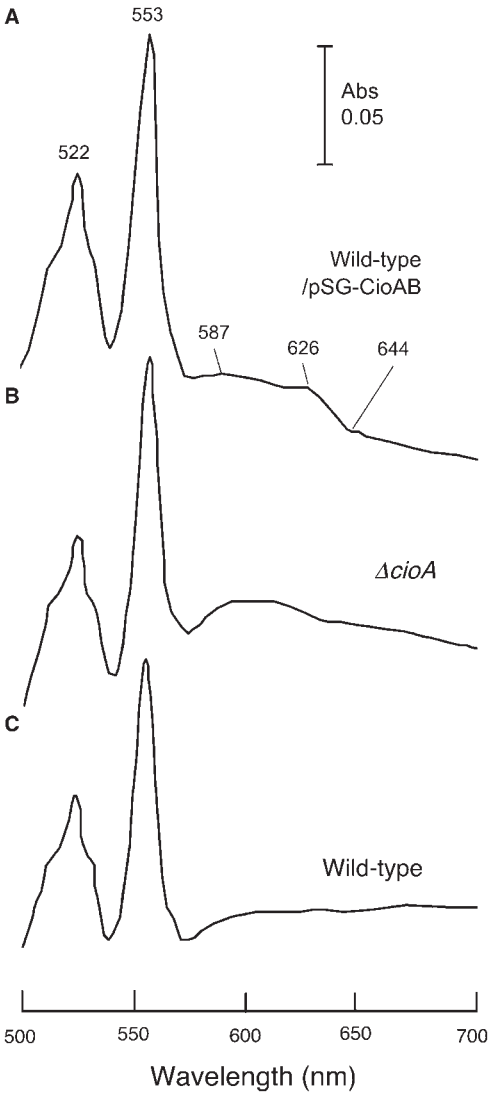

Fig. 5. **Low-temperature redox difference spectra of membranes isolated from wild-type/pSG-CioAB (A), Δ*cioA* (B) and wild-type (C).** Cells were grown in 200-ml culture up to the stationary phase (48 h) and membranes were isolated from the cells and used at 10 mg protein/ml. Hydrosulphite-reduced *minus* ferricyanide-oxidized redox difference spectra were recorded at 77 K.

Reverse-Phase HPLC/MS Analysis of Hemes—To identify heme species bound to CIO, we extracted hemes from the *G. oxydans* membranes and analysed hemes by LC/MS. In both the wild type and wild-type/pGS-CioAB, hemes were eluted at 19.6, 21.5 and 28 min with the Soret peak at 404, 398 and 394 nm, respectively, while the 19.6-min peak was absent in the Δ*cioA* mutant (Fig. 7). MS analysis identified these three peaks as heme D (chlorin), heme B (protoheme IX) and heme O with the molecular mass of 632.1, 616.0

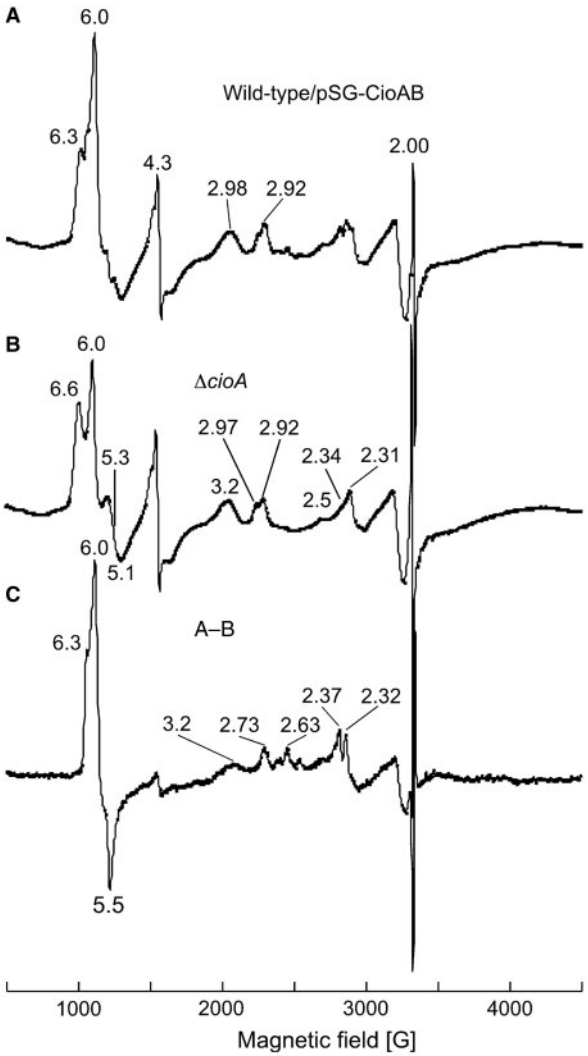

Fig. 6. **EPR spectra of *G. oxydans* wild-type/pSG-CioAB and Δ*cioA* membranes.** The difference spectra (C) was obtained by adjusting the intensity of the $g = 6.6$ signal in the traces A and B. Concentrations of the membranes were 34 mg protein/ml. EPR conditions for the traces (A) and (B) were: microwave frequency, 9.3 gHz; microwave power, 1 mW; field modulation frequency, 100 kHz; modulation amplitude, 10 G; receiver time constant, 82 ms; average scans, three times; temperature, 8.5 K.

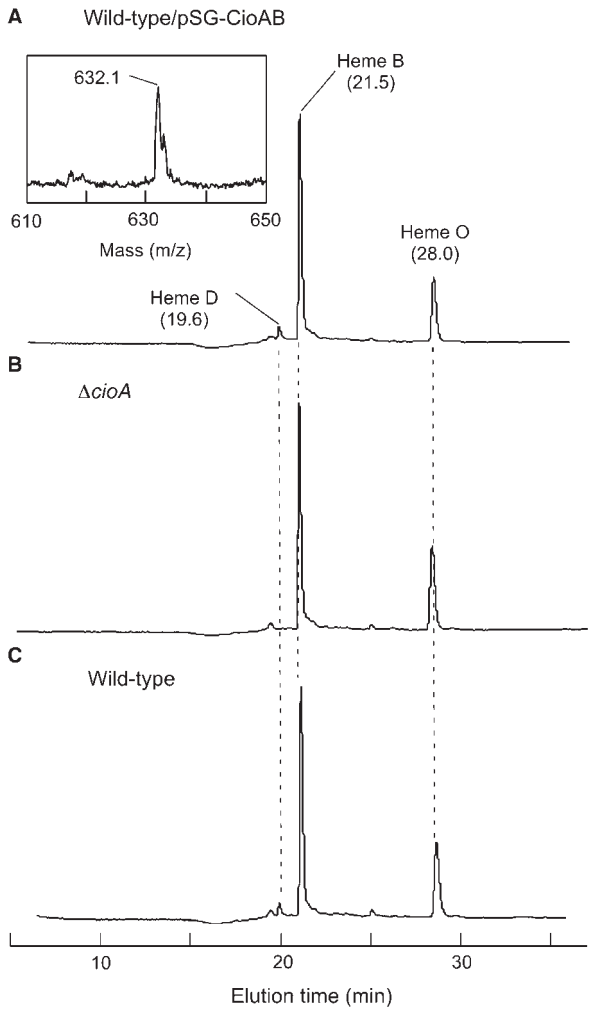

Fig. 7. **Reverse-phase HPLC chromatograms of hemes extracted from the *G. oxydans* membranes of wild-type/pSG-CioAB (A), Δ*cioA* (B) and wild-type (C).** The inset in (A) shows the ESI mass spectrum of the 19.6-min species in the mass range for heme D.

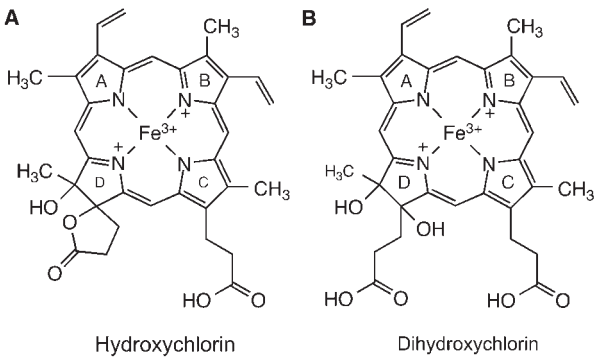

Fig. 8. **Structures of hydroxychlorin (A) and dihydroxychlorin (B).**

and 838.1 Da, respectively. The intensity of the heme D peak relative to those of hemes B and O was much less than the amount of CIO (~0.1 and ~0.2 nmol/mg protein in the wild-type and CIO-overproduced membranes, respectively). This could be due to the instability of heme D under our extraction conditions. Further, we identified the 19.6- and 21.5-min species in the membranes isolated from the *E. coli* cytochrome *bo*-deficient mutant ST4533 (Δ*cyo cyd*$^+$). These data indicate that heme D is bound to *G. oxydans* CIO. The molecular mass of the 19.6-min species indicates that heme D isolated from the *G. oxydans* and *E. coli* membranes is a hydroxychlorin with the lactonization of the ring D propionic acid (632.1 Da) (*41*) rather than a dihydroxychlorin (650.2 Da) (Fig. 8). Heme D could be formed within the oxidase by the conversion of heme B with hydrogen peroxide (*42*), which can be produced at the heme b_{595}-*d*-binding site upon reduction of the assembled enzyme.

If the efficiency of the oxidation of heme B to heme D is low in CIO, the spectroscopic identification of heme *d* in CIO would be difficult and a part of the population may remain as a heme *bbb* complex. This has to be examined in future studies with the purified CIO. It should be noted that changes in growth conditions for *Bacillus subtilis* with glucose at low aeration to without glucose at high aeration transformed cytochrome *bd* menaquinol oxidase to cytochrome *bb′* oxidase, that is fully functional and more sensitive to cyanide and aurachin D (*43*).

CONCLUSION

Because of the low expression level and the instability in detergent solution, the biochemical characterization of CIO was difficult since the discovery of CIO in *P. aeruginosa* (*9*). Here we used the *G. oxydans* CIO-overproduced membranes and obtained the spectroscopic evidence for the presence of heme b_{558}, b_{595} and *d* and the chemical evidence for the presence of heme D. Our data showed that CIO contains all three hemes present in cytochrome *bd* quinol oxidase although it has unique spectroscopic and ligand-binding properties. Sequence analysis of subunit I (CioA/CydA) (*31*) revealed the difference in the locations of prolines nearby His19 [the heme b_{595} ligand (*44*)] and Glu99 [a putative heme *d* ligand (*16*)]. Such differences could be one of the causes for the absence of spectroscopic properties and the higher cyanide resistance of CIO in the wild-type strains (*8–10*). If an unidentified ligand exits at the heme b_{595}-*d* binuclear centre of CIO, it would affect the spectroscopic and ligand-binding properties. CIO and cytochrome *bd* quinol oxidase perform a variety of physiological functions in bacteria such as the microaerophilic respiration and protection against oxygen stress (*45–47*). They also play an important role in survival and adaptation of pathogenic bacteria that encounter host environments where dioxygen is progressively limited (*48–50*). We hope that future spectroscopic studies with the purified enzyme and X-ray crystallographic studies would provide a clue for understanding the unique enzymatic and spectroscopic properties of CIO.

ACKNOWLEDGEMENTS

We thank Mr Hiroshi Miura, Ms. Chiho Kayama and Ms. Rie Taneba (Yamaguchi University) for their technical support, and also Drs Robert B. Gennis (University of Illinois), Toshiharu Yakushi (Yamaguchi University), Motonari Tsubaki (Kobe University) and Hiroshi Hori (Osaka University) for their helpful discussion.

FUNDING

A grant-in-aid for Scientific Research (20570124 to T.M. and 20658020 to K.M.); Creative Scientific Research (18GS0314 to K.K.) from the Japan Society for the Promotion of Science; and for Scientific Research on Priority Areas (18073004 to K.K.) from the Ministry of Education, Culture, Sports, Science and Technology, Japan.

CONFLICT OF INTEREST

None declared.

REFERENCES

1. Deppenmeier, U., Hoffmeister, M., and Prust, C. (2002) Biochemistry and biotechnological applications of *Gluconobacter* strains. *Appl. Microbiol. Biotechnol.* **60**, 233–242
2. Matsushita, K., Toyama, H., and Adachi, O. (1994) Respiratory chains and bioenergetics of acetic acid bacteria in *Advances in Microbial Physiology* (Rose, A.H. and Tempest, D.W., eds.) Vol. 36, pp. 247–301, Academic Press Ltd., London
3. De Ley, J., Gillis, M., and Swings, J. (1984) The genus *Gluconobacter* in *Bergey's Manual of Systematic Bacteriology* (Krieg, N.R. and Holt, J.G., eds.) Vol. 1, pp. 267–278, Williams & Wilkins, Baltimore
4. Prust, C., Hoffmeister, M., Liesegang, H., Wiezer, A., Fricke, W.F., Ehrenreich, A., Gottschalk, G., and Deppenmeier, U. (2005) Complete genome sequence of the acetic acid bacterium. *Gluconobacter oxydans. Nat. Biotechnol.* **23**, 195–200
5. Matsushita, K., Shinagawa, E., Adachi, O., and Ameyama, M. (1987) Purification and characterization of cytochrome *o*-type oxidase from *Gluconobacter suboxydans*. *Biochim. Biophys. Acta* **894**, 304–312
6. Ameyama, M., Matsushita, K., Shinagawa, E., and Adachi, O. (1987) Sugar-oxidizing respiratory chain of *Gluconobacter suboxydans*. Evidence for a branched respiratory chain and characterization of respiratory chain-linked cytochromes. *Agric. Biol. Chem.* **51**, 2943–2950
7. Adachi, O., Moonmungmee, D., Shinagawa, E., Toyama, H., Yamada, M., and Matsushita, K. (2003) New quinoprotein in oxidative fermentation. *Biochim. Biophys. Acta* **1647**, 10–17
8. Cunningham, L., Pitt, M., and Williams, H.D. (1997) The *cioAB* genes from *Pseudomonas aeruginosa* code for a novel cyanide-insensitive terminal oxidase related to the cytochrome *bd* quinol oxidases. *Mol. Microbiol.* **24**, 579–591
9. Matsushita, K., Yamada, M., Shinagawa, E., Adachi, O., and Ameyama, M. (1983) Membrane-bound respiratory chain of *Pseudomonas aeruginosa* grown aerobically. A KCN-insensitive alternate oxidase chain and its energetics. *J. Biochem.* **93**, 1137–1144
10. Jackson, R.J., Elvers, K.T., Lee, L.J., Gidley, M.D., Wainwright, L.M., Lightfoot, J., Park, S.F., and Poole, R.K. (2007) Oxygen reactivity of both respiratory oxidases in *Campylobacter jejuni*: the *cydAB* genes encode a cyanide-resistant, low-affinity oxidase that is not of the cytochrome *bd* type. *J. Bacteriol.* **189**, 1604–1615
11. Cunningham, L. and Williams, H.D. (1995) Isolation and characterization of mutants defective in the cyanide-insensitive respiratory pathway of *Pseudomonas aeruginosa*. *J. Bacteriol.* **177**, 432–438
12. Blumer, C. and Haas, D. (2000) Mechanism, regulation, and ecological role of bacterial cyanide biosynthesis. *Arch. Microbiol.* **173**, 170–177
13. Goldfarb, W.B. and Margraf, H. (1967) Cyanide production by *Pseudomonas aeruginosa*. *Ann. Surg.* **165**, 104–110
14. Zlosnik, J.E.A., Tavankar, G.R., Bundy, J.G., Mossialos, D., O'Toole, R., and Williams, H.D. (2006) Investigation of the physiological relationship between the cyanide-insensitive oxidase and cyanide production in *Pseudomonas aeruginosa*. *Microbiology* **152**, 1407–1415
15. Tonouchi, N., Sugiyama, M., and Yokozeki, K. (2003) Construction of a vector plasmid for use in *Gluconobacter oxydans*. *Biosci. Biotechnol. Biochem.* **67**, 211–213
16. Mogi, T., Endo, S., Akimoto, S., Morimoto-Tadokoro, M., and Miyoshi, H. (2006) Glutamates 99 and 107 in

transmembrane helix III of subunit I of cytochrome *bd* are critical for binding of the heme b_{595}-*d* binuclear center and enzyme activity. *Biochemistry* **45**, 15785–15792
17. Tsubaki, M., Mogi, T., Anraku, Y., and Hori, H. (1993) Structure of heme-copper binuclear center of the cytochrome *bo* complex of *Escherichia coli*: EPR and Fourier-transform infrared spectroscopic studies. *Biochemistry* **32**, 6065–6072
18. Cheng, Y.C. and Prusoff, W.H. (1973) Relationship between the inhibition constant (K_I) and the concentration of inhibitor which cause 50 per cent inhibition (I_{50}) of an enzymatic reaction. *Biochem. Pharmacol.* **22**, 3099–3108
19. Matsumoto, Y., Muneyuki, E., Fujita, D., Sakamoto, K., Miyoshi, H., Yoshida, M., and Mogi, T. (2006) Kinetic mechanism of quinol oxidation by cytochrome *bd* studied with ubiquinone-2 analogs. *J. Biochem.* **139**, 779–788
20. Sootsuwana, K., Lertwattanasakula, N., Thanonkeob, P., Matsushita, K., and Yamada, M. (2008) Analysis of the respiratory chain in ethanologenic *Zymomonas mobilis* with a cyanide-resistant *bd*-type ubiquinol oxidase as the only terminal oxidase and its possible physiological roles. *J. Mol. Microbiol. Biotechnol.* **14**, 163–175
21. Weinstein, J.D. and Beale, S.I. (1983) Separate physiological roles and subcellular compartments for two tetrapyrrole biosynthetic pathways in *Euglena gracili*. *J. Biol. Chem.* **258**, 6799–6807
22. Miyoshi, H., Takegami, K., Sakamoto, K., Mogi, T., and Iwamura, H (1999) Characterization of the ubiquinol oxidation sites in cytochromes *bo* and *bd* from *Escherichia coli* using aurachin C analogues. *J. Biochem.* **125**, 138–142
23. Sakamoto, K., Miyoshi, H., Takegami, K., Mogi, T., Anraku, Y., and Iwamura, H. (1996) Probing substrate binding site of the *Escherichia coli* quinol oxidases using synthetic ubiquinol analogues based upon their electron-donating efficiency. *J. Biol. Chem.* **271**, 29897–29902
24. Mogi, T., Tsubaki, M., Hori, H., Miyoshi, H., Nakamura, H., and Anraku, Y. (1998) Two terminal quinol oxidase families in *Escherichia coli*: Variations on molecular machinery for dioxygen reduction. *J. Biochem. Mol. Biol. Biophys.* **2**, 79–110
25. Mogi, T., Akimoto, S., Endou, S., Watanabe-Nakayama, T., Mizuochi-Asai, E., and Miyoshi, H. (2006) Probing the ubiquinol-binding site in cytochrome *bd* by site-directed mutagenesis. *Biochemistry* **45**, 7924–7930
26. Sato-Watanabe, M., Mogi, T., Miyoshi, H., Iwamura, H., Matsushita, K., Adachi, O., and Anraku, Y. (1994) Structure-function studies on the ubiquinol oxidation site of the cytochrome *bo* complex from *Escherichia coli* using *p*-benzoquinones and substituted phenols. *J. Biol. Chem.* **269**, 28899–28907
27. Ui, H., Ishiyama, A., Sekiguchi, H., Namatame, M., Nishihara, A., Takahashi, A., Shiomi, K., Otoguro, K., and Ōmura, S. (2007) Selective and potent *in vitro* antimalarial activities found in four microbial metabolites. *J. Antibiot.* **60**, 220–222
28. Jünemann, S. and Wrigglesworth, J.M. (1994) Antimycin inhibition of the cytochrome *bd* complex from *Azotobacter vinelandii* indicates the presence of a branched electron transfer pathway for the oxidation of ubiquinol. *FEBS Lett.* **345**, 198–202
29. Mogi, T., Ui, H., Shiomi, K., Ōmura, S., and Kita, K. (2008) Gramicidin S identified as a potent inhibitor for cytochrome *bd*-type quinol oxidase. *FEBS Lett.* **582**, 2299–2302
30. Mogi, T., Ui, H., Shiomi, K., Ōmura, S., Miyoshi, H., and Kita, K. (2009) Antibiotics LL-Z1272 identified as novel inhibitors discriminating bacterial and mitochondrial quinol oxidases. *Biochim. Biophys. Acta* **1787**, 129–133
31. Mogi, T. and Miyoshi, H. (2009) Characterization of cytochrome *bd* plasoquinol oxidase from the cyanobacterium *Synechocystis* sp. PCC 6803. *J. Biochem.* **145**, 395–401
32. Minagawa, N., Yabu, Y., Kita, K., Nagai, N., Ohta, N., Meguro, K., Sakajo, S., and Yoshimoto, A. (1997) An antibiotic, ascofuranone, specifically inhibits respiration and *in vitro* growth of long slender bloodstream forms of *Trypanosoma brucei brucei*. *Mol. Biochem. Parasitol.* **84**, 271–280
33. Matsushita, K., Yakushi, T., Toyama, H., Shinagawa, E., and Adachi, O. (1996) Function of multiple heme c moieties in intramolecular electron transport and ubiquinone reduction in the quinohemoprotein alcohol dehydrogenase-cytochrome c complex of *Gluconobacter suboxydans*. *J. Biol. Chem.* **271**, 4850–4857
34. Kita, K., Konishi, K., and Anraku, Y (1984) Terminal oxidases of the *Escherichia coli* aerobic respiratory chain. II. Purification and properties of the cytochrome *bd* complex from cells grown with limited oxygen and evidence of branched electron-carrying systems. *J. Biol. Chem.* **259**, 3375–3381
35. DerVartanian, D.V., Iburg, L.K., and Morgan, T.V. (1973) EPR studies on phosphorylating particles from *Azotobacter vinelandii*. *Biochim. Biophys. Acta* **305**, 173–178
36. Poole, R.K. and Williams, H.D. (1987) Proposal that the function of the membrane-bound cytochrome a_1-like haemoprotein (cytochrome *b*-595) in *Escherichia coli* is a direct electron donation to cytochrome *d*. *FEBS Lett.* **217**, 49–52
37. Hata-Tanaka, A., Matsuura, K., Itoh, S., and Anraku, Y. (1987) Electron flow and heme-heme interaction between cytochromes *b*-558, *b*-595 and *d* in a terminal oxidase of *Escherichia coli*. *Biochim. Biophys. Acta* **893**, 289–295
38. Meinhard, S.W., Gennis, R.B., and Ohnishi, T. (1989) EPR properties of the cytochrome-*d* complex of *Escherichia coli*. *Biochim. Biophys. Acta* **975**, 175–184
39. Hata, A., Kirino, Y., Matsuura, K., Itoh, S., Hiyama, T., Kinishi, K., Kita, K., and Anraku, Y. (1985) Assignment of ESR signals of *Escherichia coli* terminal oxidase complexes. *Biochim. Biophys. Acta* **810**, 62–72
40. Tsubaki, M., Hori, H., Mogi, T., and Anraku, Y. (1995) Cyanide-binding site of *bd*-type ubiquinol oxidase from *Escherichia coli*. *J. Biol. Chem.* **270**, 28565–28569
41. Timkovich, R., Cork, M.S., Gennis, R.B., and Johnson, P.Y. (1985) Proposed structure of heme *d*, a prosthetic group of bacterial terminal oxidases. *J. Am. Chem. Soc.* **107**, 6069–6075
42. Sugiyama, K., Highet, R.J., Woods, A., Cotter, R.J., and Osawa, Y. (1997) Hydrogen peroxide-mediated alteration of the heme prosthetic group of metmyoglobin to an iron chlorin product: Evidence for a novel oxidative pathway. *Proc. Natl Acad. Sci. USA* **94**, 796–801
43. Azarkina, N., Siletsky, S., Borisov, V., von Wachenfeldt, C., Hederstedt, L., and Konstantinov, A.A. (1999) A cytochrome *bb′*-type quinol oxidase in *Bacillus subtilis* strain 168. *J. Biol. Chem.* **274**, 32810–32817
44. Fang, G.H., Lin, R.J., and Gennis, R.B. (1989) Location of heme axial ligands in the cytochrome *d* terminal oxidase complex of *Escherichia coli* determined by site-directed mutagenesis. *J. Biol. Chem.* **264**, 8026–8032
45. D'Mello, R., Hill, S., and Poole, R.K. (1996) The cytochrome *bd* quinol oxidase in *Escherichia coli* has an extremely high oxygen affinity and two oxygen binding haems: implications for regulation of activity *in vivo* by oxygen inhibition. *Microbiology* **142**, 755–763
46. Smith, A., Hill, S., and Anthony, C. (1990) The purification, and characterization and role of the *d*-type cytochrome oxidase of *Klebsiella pneumoniae* during nitrogen fixation. *J. Gen. Microbiol.* **136**, 171–180
47. Baughn, A.D. and Malamy, M.H. (2004) The strict anaerobe *Bacteroides fragilis* grows in and benefits from nanomolar concentrations of oxygen. *Nature* **427**, 441–444
48. Shi, L., Sohaskey, C.D., Kana, B.D., Dawes, S., North, R.J., Mizrahi, V., and Gennaro, M.L. (2005) Changes in

energy metabolism of *Mycobacterium tuberculosis* in mouse lung and under *in vitro* conditions affecting aerobic respiration. *Proc. Natl Acad. Sci. USA* **102**, 15629–15634

49. Way, S.S., Sallustio, S., Magliozzo, R.S., and Goldberg, M.B. (1999) Impact of either elevated or decreased levels of cytochrome *bd* expression on *Shigella flexneri* virulence,. *J. Bacteriol.* **181**, 1229–1237
50. Endley, S., McMurray, D., and Ficht, T.A. (2001) Interruption of the *cydB* locus in *Brucella abortus* attenuates intracellular survival and virulence in the mouse model of infection. *J. Bacteriol.* **183**, 2454–2462